# New Magnetotransport Phenomenon in a Two-Dimensional Electron Gas in the Presence of a Weak Periodic Submicrometer Potential

*D. Weiss*[1], *K. v. Klitzing*[1], *K. Ploog*[1], *and G. Weimann*[2]

[1]Max-Planck-Institut für Festkörperforschung, Heisenbergstr. 1, D-7000 Stuttgart 80, Fed. Rep. of Germany

[2]Walter-Schottky-Institut, TUM, D-8046 Garching, Fed. Rep. of Germany

A new type of magnetoresistance oscillation periodic in 1/B is observed when the carrier density $N_s$ of a two-dimensional electron gas is weakly modulated with a period smaller than the mean free path of the electrons. In high mobility AlGaAs-GaAs heterojunctions the carrier density is periodically modulated by illumination of the samples with two interfering laser beams at liquid helium temperatures. The modulation arises due to the persistent photoconductivity of the samples at low temperatures. The experiments show that the period of the additional quantum oscillation is determined by the separation $a$ of the interference fringes. This period corresponds to Shubnikov-de Haas oscillations where only the electrons within the first reduced Brillouin zone with $|k| < \pi/a$ contribute.

## 1. Introduction

At low temperatures the magnetoresistance of a degenerate two-dimensional electron gas (2-DEG) exhibits the well-known Shubnikov-de Haas (SdH) oscillations periodic in 1/B. Lateral confinement of the 2-DEG on a submicrometer scale leads to deviations from the typical 1/B periodicity of these SdH-oscillations [1]. Within a naive picture these deviations occur when the cyclotron orbit of an electron is larger than the width of the confining potential [2]. An intermediate situation between a purely two-dimensional system and a quasi-one-dimensional quantum wire arises if the confining potential of the quantum wire is replaced by a weaker periodic potential with a length scale smaller than the mean free path of the electrons. The experiments show that under this condition a new type of magnetoresistance oscillation becomes visible with a periodicity depending on the period of the superimposed potential.

In selectively doped AlGaAs-GaAs heterostructures a persistent increase in the two-dimensional electron density is observed at temperatures below T=150K if the device is illuminated with infrared or visible light. This phenomenon is usually explained on the basis of the properties of DX-centers which seem to be related to a deep Si donor [3]. The increase in the electron density depends on the photon flux absorbed in the semiconductor so that a spatially modulated photon flux generates a modulation in the carrier density. In our measurements a holographic illumination of the heterostructure at liquid helium temperatures is used to produce a periodic potential with a period on the order of the wavelength of the interfering beams. In Fig.1 the interference of two plane light waves which create a periodic modulation of the ionized donors and therefore of the carrier density is shown schematically.

The existence of a periodically modulated carrier density in such structures has been demonstrated by Tsubaki, Sakaki, Yoshino, and Sekiguchi [4] who measured the anisotropy of the resistivity parallel and perpendicular to the interference fringes at 90K. Tsubaki and coworkers stated that the smallest possible period for finding an anisotropic resistivity is four or five times as large as the thickness of the AlGaAs layers on top of the 2-DEG. Since we have created smaller fringe periods we have observed nearly isotropic resistivity at zero magnetic field. In the presence of a magnetic field,

Springer Series in Solid-State Sciences, Vol. 87
**High Magnetic Fields in Semiconductor Physics II** Editor: G. Landwehr

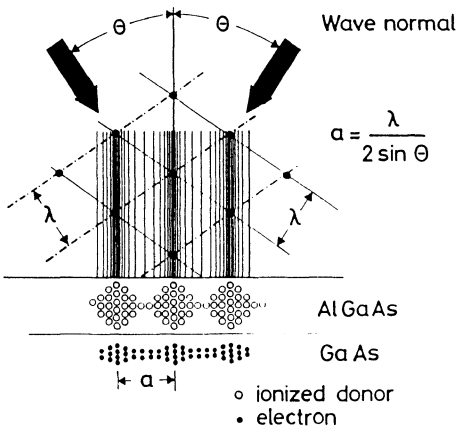


Figure 1: Sketch of the spatial modulation of the concentration of ionized donors in the AlGaAs layer and of electrons in the 2-DEG produced by holographic illumination using two interfering laser beams with wavelength $\lambda$. The interference pattern created is shown schematically

however, a new oscillatory phenomenon occurs demonstrating clearly that a periodic modulation of the 2-DEG is present.Details will be given in the following sections.

## 2. Experimental

The samples used in the experiments were conventional AlGaAs-GaAs heterostructures grown by molecular beam epitaxy [5] with carrier densities between $1.5 \cdot 10^{11}\text{cm}^{-2}$ and $4.3 \cdot 10^{11}$ $\text{cm}^{-2}$ and low temperature mobilities ranging from $0.23 \cdot 10^{6}\text{cm}^2/\text{Vs}$ to $1 \cdot 10^{6}\text{cm}^2/\text{Vs}$. Illumination of the samples increases both the carrier density and the mobility at low temperatures. The heterojunctions discussed in the following sections consist of a semi-insulating GaAs substrate, followed by a $1\mu\text{m}-4\mu\text{m}$ thick undoped GaAs buffer layer, an undoped AlGaAs spacer (6nm-33nm), Si-doped AlGaAs (33nm-84nm), and an undoped GaAs toplayer ($\approx$ 22nm). We have chosen an L-shaped geometry (sketched on the right hand side of Fig.2) to investigate the magnetotransport properties parallel and perpendicular to the interference fringes. Such a mesa structure was produced using standard photolithographic and etch techniques. Ohmic contacts to the 2-DEG were formed by alloying AuGe/Ni layers at 450°C. Some of the samples investigated have an evaporated semi-transparent NiCr front gate (thickness $\approx$ 8nm) or a back gate, respectively, in order to vary the carrier density after holographic illumination.

The experiment was carried out using either a 5mW HeNe laser ($\lambda$ = 633nm) or a 3mW Argon-Ion laser ($\lambda$ = 488nm) both linearly polarized. The experimental realization of the holographic illumination is shown schematically on the left hand side of Fig.2. The laser system was mounted on top of the sample holder which was immersed in liquid helium (4.2K) within a 10-Tesla magnet system. The laser beam which was expanded to a diameter of 40mm entered the sample holder through a quartz window and a shutter. The shutter ensures well-defined illumination times of the sample down to 25ms. Short exposure times are important to prevent jumping of the fringes; therefore exposure times between 25ms and 100ms were typically chosen. The mirrors which split the laser beam into two coherent waves, are located close to the device and are arranged in such a way that an interference pattern with a period $a$ is generated at the surface of the device. An aperture mounted above covers the sample from direct illumination. The period $a$ of the fringes created in this way depends on the wavelength $\lambda$ of the laser and the incident angle $\Theta$ (see Fig.1): $a = \lambda/2sin\Theta$. With the wavelengths used in this experiment and $\Theta = 56^o$ we obtain periods of 382nm and 294nm for the interference pattern. Care was taken to minimize stray light originating from components inside

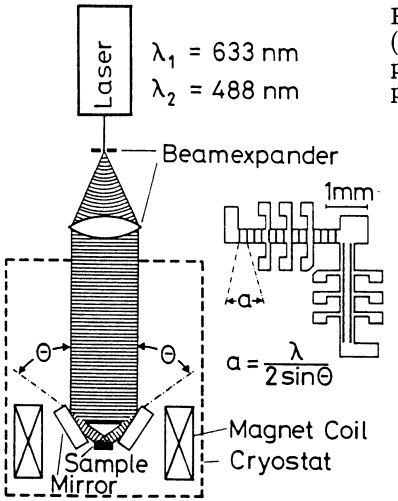


Figure 2: Schematic experimental set-up (left hand side) and top view of the L shaped sample geometry where the interference pattern is sketched

the sample holder by coating them with an absorbing layer. In order to reduce wavefront distortion due to rough surfaces of the optical components, all mirrors, lenses, and windows have a high quality polished surface. The wavefront distortion specification of these components is better than $\lambda/10$ where $\lambda$ is the wavelength of a HeNe-laser ($\lambda = 633$nm).

## 3. Magnetotransport Measurements

After holographic illumination of the sample which was carried out at 4.2K we have measured the resistivities $\rho_\perp$ (pependicular to the interference fringes) and $\rho_{||}$ (parallel to the fringes) at cryogenic temperatures as a function of the magnetic field. The magnetic field was perpendicular to the plane of the 2-DEG. In addition, the Hall resistances $R_H^\perp$ and $R_H^{||}$ have been measured. The use of the indices $\perp$ and $||$ is illustrated in Fig.3. The resistivities and Hall resistances are measured applying a constant current ($1\mu$m$-10\mu$m) and measuring the voltage drop between potential probes along and perpendicular to the direction of current flow, respectively. A typical result obtained for a fringe period of $a$ =382nm is shown in Fig.3. At magnetic fields above 0.5T both $\rho_\perp$ and $\rho_{||}$ show the well known SdH-oscillations with a periodicity $\Delta(1/B)$ inversely proportional to the 2-DEG carrier density $N_s$. Below 0.5T pronounced additional oscillations dominate $\rho_\perp$ while weaker oscillations with a phase shift of 180° relative to the $\rho_\perp$ data are visible in the $\rho_{||}$ measurements. The oscillations in $\rho_\perp$ are accompanied by a remarkable positive magnetoresistance at very low magnetic fields. The Hall resistances ,however, show no additional structure at magnetic fields below 0.5T even at the highest resolution used. Deviations from the clear linear behaviour of $R_H^\perp$ and $R_H^{||}$ occur only at magnetic fields above 0.5T, and are connected to the SdH oscillations starting to be resolved. The slightly different slopes of $R_H^\perp$ and $R_H^{||}$ are due to a small difference in the carrier density of about 4%. The additional oscillations in $\rho_\perp$ and $\rho_{||}$ are perfectly periodic in 1/B. This is demonstrated in the inset of Fig.4 where the oscillation index $m$ is plotted versus the inverse magnetic field. The points in the inset correspond to minima in $\rho_\perp$. The oscillations in Fig.4 are obtained for a fringe period of 382nm. The behaviour of

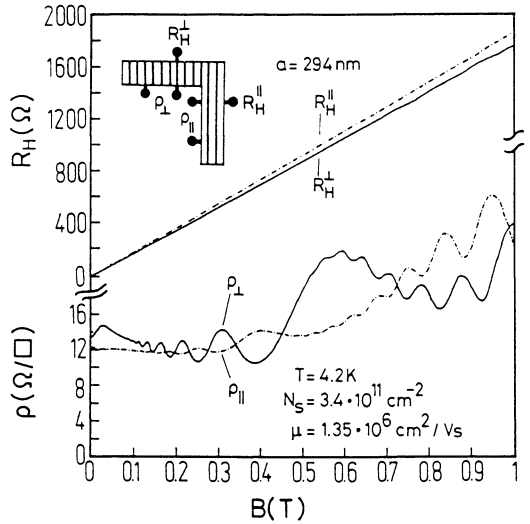


Figure 3: Magnetoresistivity $\rho$ and Hall resistance $R_H$ parallel and perpendicular to the interference fringes. The inset defines the use of the indices $\perp$ and $\parallel$ with respect to the interference fringes shown schematically

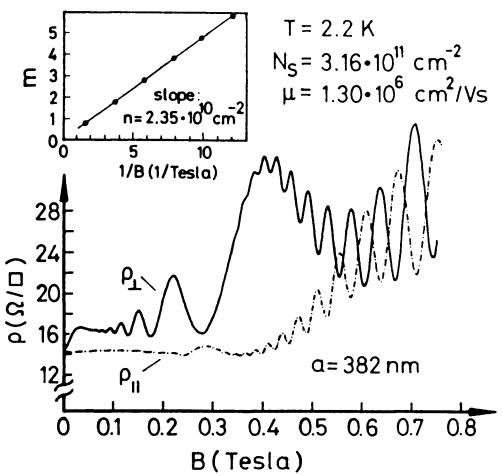


Figure 4: Magnetoresistivity $\rho$ parallel and perpendicular to the interference fringes. The inset displays the 1/B dependence of the additional oscillations where the points correspond to minima in $\rho_\perp$

these additional oscillations of $\rho_\perp$ and $\rho_\parallel$ as displayed in Fig.4 is essentially the same as those shown in Fig.3. Since the additional oscillations in $\rho_\perp$ are perfectly periodic in 1/B the periodicity can be expressed as a carrier density $n$. Analogous to SdH-oscillations one obtains (spin splitting not resolved)

$$n = \frac{e}{\pi\hbar}(\Delta\frac{1}{B})^{-1} \quad . \tag{1}$$

Here $e$ is the elementary charge, $\hbar$ is Planck's constant and $\Delta(1/B)$ is the difference between adjacent minima (or maxima) of $\rho_\perp$ or $\rho_\parallel$ on a 1/B scale. The additional oscillations in Fig.4 correspond to a carrier density $n = 2.35 \cdot 10^{10}\text{cm}^{-2}$ while the periodicity

of $\rho_\perp$ in Fig.3 gives $n = 3.2 \cdot 10^{10}\text{cm}^{-2}$. This result suggests that a shorter period $a$ results in higher values for $n$ as long as the carrier densities $N_s$ are approximately equal.

Up to now we have not completely ruled out the possibility that the additional oscillatory structures are due to an occupation of the next higher subband. Temperature dependent measurements of $\rho_\perp$ shown in Fig.5 demonstrate that the additional oscillations are much less temperature dependent than SdH oscillations. The SdH oscillations have a strong temperature dependence since their amplitudes depend on the Landau level seperation $\hbar\omega_c$ as compared to the thermal energy $k_BT$. Therefore the additional oscillations do not originate from the Landau level seperation $\hbar\omega_c$ as one would expect also for electrons in higher subbands.

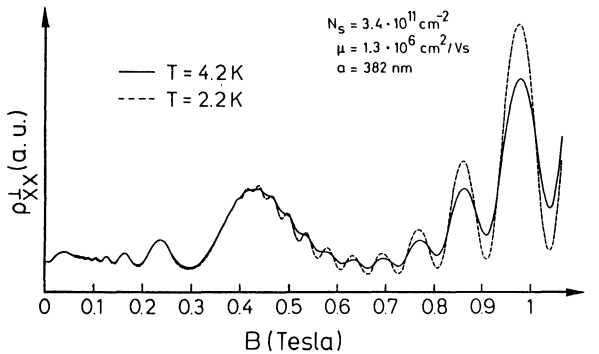


Figure 5: $\rho_\perp$ versus B for two temperatures. The SdH oscillations exhibit the expected strong temperature dependence, while the additional oscillations remain nearby unchanged for a change in temperature of 2K

By means of Fig.6 we wish to demonstrate that the additional oscillations are due to the existence of a periodically modulated charge pattern. After the first holographic illumination of the sample, $\rho_\perp$ displays pronounced additional oscillations. The interference pattern created by a second illumination should be shifted with respect to the first one due to vibrations of the experimental set up. The periodic modulation should therefore be smeared out and the additional oscillatory structure should disappear. This effect is visible in Fig.6 where the amplitude of the additional oscillations is drastically reduced after a second illumination with 500ms duration. We have found that continous

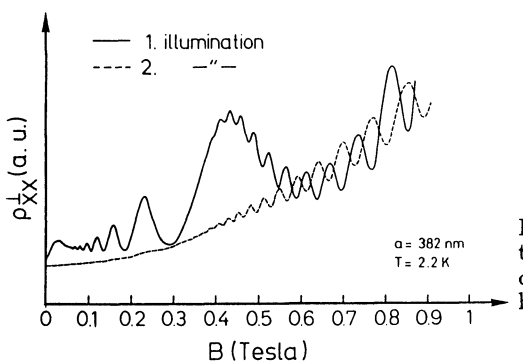


Figure 6: $\rho_\perp$ versus B. The amplitude of the additional oscillation is drastically reduced after a second holographic illumination

illumination always destroys the oscillations indicating that a proper fringe pattern is essential for observing the effect.

From the SdH-oscillations (using Eq.1) as well as from low field Hall measurements an average carrier density $N_s$ of the periodically modulated 2-DEG can be obtained. The carrier density $N_s$ and mobility $\mu$ we have measured parallel and perpendicular to the interference pattern are equal within 5%. Since, in addition, we do not observe additional structure in the higher magnetic field regime of $\rho_\perp$ and $\rho_\parallel$ due to a second carrier density, we conclude that we have only a weak modulation of the carrier density. This means that the amplitude of the additional periodic potential introduced by holographic illumination is small compared to the Fermi energy of the system. A stronger potential modulation, achievable e.g. by holographic illumination of a photoresist coated sample and followed by suitable etching techniques leads to a clear anisotropy of the resistivity parallel and perpendicular to the grating [8].

The period of the additional oscillations depends on the carrier density $N_s$. This is shown in Fig.7 where the carrier density has been varied after holographic illumination. The data in Fig.7 were obtained applying a voltage to a semi-transparent gate on top of the sample. Changing the carrier density $N_s$ results in a change of the periodicity of the additional oscillations in $\rho_\perp$ and $\rho_\parallel$; as $N_s$ increases, $\Delta(1/B)$ decreases and therefore $n$ increases, too. In Fig.7 less additional oscillations are resolved compared to the magnetoresistivity data shown i.e. in Fig.4. This we contribute to the lower mobility of the sample and will be discussed within the next section.

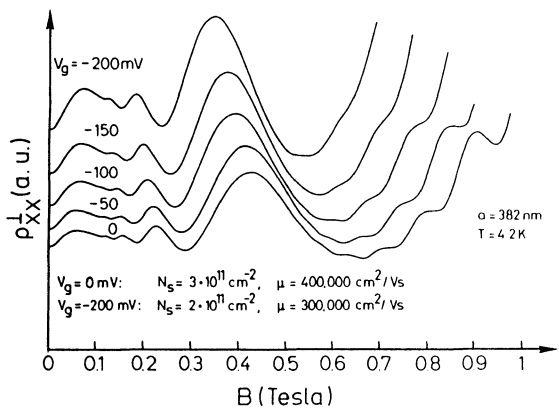


Figure 7: Gate voltage dependence of the magnetoresistivity $\rho_\perp$. Reducing the carrier density $N_S$ results in an increasing $\Delta(1/B)$ value and therefore in a reduced carrier

## 4. Discussion

The experiments described in the previous sections have been carried out using samples with different mobilities and carrier densities. In addition we have changed the carrier density applying a voltage to a front- or backgate, we have varied the illumination times and we have used two periods $a$=294nm and $a$=382nm, respectively. Nevertheless, the results can be summarized in a simple plot. In Fig.8 the carrier density $n$ determined by the periodicity (Eq.1) of the additional oscillations is plotted as a function of the carrier density $N_s$. The lines in Fig.8 are calculated curves without any free parameter based on the assumption that the period is simply given by the condition that the classical cyclotron orbit is equal to an integer number of fringe periods $a$ (visualized in the inset of Fig.8):

$$R_c = \frac{m^*}{e}\frac{v_F}{B} = \frac{a}{2}(m+\varphi) \qquad m = 1,2,3,\ldots \quad . \tag{2}$$

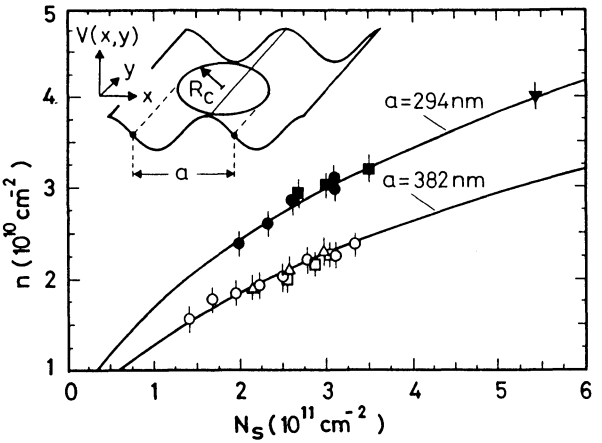


Figure 8: $n$ versus $N_s$. Full symbols correspond to a laser wavelength $\lambda$=488nm, open symbols to $\lambda$=633nm and different symbols represent different samples. The solid lines are calculated using the condition that the cyclotron orbit diameter $2R_c$ is equal to an integer multiple of the interference period $a$, as sketched in the inset

$R_c$ is the cyclotron radius, $v_F$ is the electron velocity at the Fermi energy, $m^*$ is the electron effective mass and $\varphi$ is a phase factor. Substituting for $v_F$ using $v_F = \hbar k_F/m^*$ we can rewrite Eq.2 to obtain

$$\Delta\frac{1}{B} = e\frac{a}{2\hbar k_F} \tag{3}$$

calculating $n$ using Eq.1 and the relation $k_F = (2\pi N_s)^{1/2}$.

$$n = \frac{2k_F}{\pi a} \quad . \tag{4}$$

This simple picture is in excellent agreement with the experimental data. The model described above requires an elastic free path $l_e$ at least as long as the perimeter of the cyclotron orbit. This agrees with our finding that the number of oscillation periods depends on the mobility of the sample; the higher the mobility the more oscillations are observable. From the mobility of the sample used in the measurements of Fig.4 a mean free path of 12$\mu$m can be calculated in agreement with the estimated cyclotron orbit perimeter of 11$\mu$m for the largest cyclotron orbit which produces a structure in the $\rho_\perp$ curve at about 0.054T ($m$=9 in Fig.4). If maxima in the $\rho_\perp$ curves are interpreted as maxima in the scattering rate then the experimentally determined phase shift $\varphi$=0.17$\pm$0.06 in Eq.4 implies that the strongest interaction of the cyclotron motion with the periodic potential occurs if the diameter of the cyclotron orbit is 0.17$a$ larger than an integer multiple of the period $a$. On the other hand minima occur when $\varphi$=$-$0.25$\pm$0.06. It should be mentioned that this effect seems to be similar to the magnetoacoustic resonance [6,7]; the detailed mechanism however which results in minima in $\rho_\perp$ while at the same magnetic field $\rho_{||}$ displays maxima can not be explained within this picture at the moment.

The period of the additional oscillations can be described in a more quantum mechanical picture. The additional periodic potential introduces a new reduced Brillouin zone scheme with the period of the reciprocal lattice vector $2\pi/a$. This is illustrated in

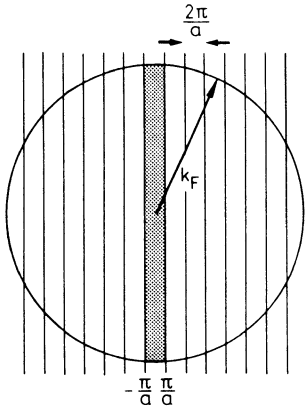


Figure 9: New Brillouin zone structure obtained by superimposing a one-dimensional periodic potential with period $a$ on a free 2-DEG. The states in the first Brillouin zone are displayed shaded. The carrier density required to fill the first Brillouin zone is equal to the carrier density $n$ deduced from the additional oscillations

Fig.9 where the first Brillouin zone is displayed shaded. Since $\pi/a$ is small compared to $k_F$ in our system, the area $A$ (in k-space) of the occupied states in the first Brillouin zone is given to good approximation by

$$A = 4k_F\frac{\pi}{a} \quad . \tag{5}$$

The carrier density $n$ required to fill the first Brillouin zone can now easily be calculated bearing in mind that one state in k-space occupies the area $(2\pi/L)^2$ (L = length of the sample) and that each state can be occupied by two electrons with opposite spin:

$$n = N/L^2 = \frac{2k_F}{\pi a} \quad . \tag{6}$$

This result is the same as that which we have already obtained in Eq.4. Our finding is that the carrier density which fills the first reduced Brillouin zone is equal to that connected with the additional oscillations. Equation 6 describes correctly the experimentally observed periodicity, however, without explaining the mechanism leading to the oscillatory behaviour of $\rho_\perp$ and $\rho_\parallel$. The solution of this problem may be connected to the magnetic breakdown [9],[10].

## 5. Summary

In summary we have reported a new type of magnetoresistance oscillation, the periodicity of which can be equally well described either by the condition that the classical cyclotron orbit equals an integer multiple of the periodic potential period or in terms of the carrier density required to fill the first reduced Brillouin zone of the modulated system. The detailed mechanism, however, which leads to the additional oscillatory structure remains to be solved.

## 6. Acknowledgements

We would like to thank D. Heitmann for stimulating suggestions and R. R. Gerhardts, A. MacDonald, P. Středa, and S. Bending for very helpful discussions.

## 7. References


[1] K.-F. Berggren, T. J. Thornton, D. J. Newson, M. Pepper *Phys.Rev.Lett.* **57**, 1769 (1986)

[2] H. van Houten, B. J. van Wees, E. J. Mooij, G. Roos, K.-F. Berggren *Superlattices and Microstructures* **3**, 497 (1987)

[3] E. F. Schubert, J. Knecht, K. Ploog, *J.Phys.* **C18**, L215 (1985)

[4] K. Tsubaki, H. Sakaki, J. Yoshino, Y. Sekiguchi *Appl. Phys. Lett.* **45**, 663 (1984)

[5] E. F. Schubert, K. Ploog, *Appl. Phys.* **A33**, 63 (1984)

[6] A. B. Pippard *Phil. Mag.* **2**, 1147 (1957)

[7] M. H. Cohen, M. J. Harrison, W. A. Harrison *Phys. Rev.* **117**, 937 (1960)

[8] M. Hundhausen, T. Ichiguchi, Y. Shiraki *Appl. Phys. Lett.* **53**, 110 (1988)

[9] M. H. Cohen, L. Falicov *Phys. Rev. Lett.* **7**, 231 (1961)

[10] A. MacDonald & P.Středa private communication